Modeling on Urban Land Use Characteristics and Urban System of the Traditional Chinese Era (1930s) Based on the Historical Military Topographic Map

Zhiwei Wan [1,2] **and Hongqi Wu** [1,*]

1 Department of History, Jinan University, Guangzhou 510632, China
2 School of Geography and Environmental Engineering, Gannan Normal University, Ganzhou 341000, China
* Correspondence: twhq@jnu.edu.cn

Abstract: The quantitative urban system structure in historical periods and the long time-scale urban land area grid dataset with spatial attributes are important for land use and land cover change (LUCC) research. In this study, we aimed to measure the area of county level and above cities in mainland China in the 1930s, also known as the traditional Chinese era (TCE), using a geographic information system (GIS) model and 1:50,000 military topographic maps. Furthermore, we aimed to identify the structure and characteristics of the urban system in the TCE according to the administrative area division using methods such as the rank size law. The results of this study revealed that 1265 county level and above cities existed in the TCE, including 25 provincial level or above cities, 179 prefectural level cities, and 1061 county level cities. The total land area of all of the cities was 1396.48 km^2, with a mean value of 1.1 km^2 and a standard deviation of 2.37 km^2. The rank-size analysis indicated that the urban system in TCE was characterized by large cities with insignificant development ($q = 0.829 < 1$, $R^2 = 0.905$). The results of the Lorenz curve and Moran analyses showed that the spatial distribution of the urban systems in China during the traditional period exhibited nonuniform agglomeration. Large-scale military topographic maps of historical periods have proven to be a good source for land use reconstruction. The $1° × 1°$ grid urban land area dataset constructed based on a GIS model in the TCE is important for future research on historical LUCC and can provide basic data for climate change models, urban economic history, and other disciplines.

Keywords: historic land use; traditional Chinese era; urban systems; urban land use; historic topographic map

1. Introduction

The urban built-up area is one of the major types of land use and land cover change (LUCC), and it is also the land use type that has most drastically changed the morphology of the Earth's surface [1,2]. With the development of human civilization [3,4], the human factor now plays an increasingly significant role in LUCC [5,6]. Historical land use datasets with geospatial attributes are required for making future LUCC projections and for climate change modelling. Several research programs organized by the international scientific community since the 1990s, such as the International Human Dimensions Programme on Global Environmental Change (IHDP) [7,8] and the International Geosphere Biosphere Project (IGBP) [9], have enhanced the reconstruction of the historical LUCC [10]. Driven by frameworks such as the IGBP/BIOME300 and past global changes (PAGES) [11,12], the quantitative reconstruction of the spatial patterns and evolutionary processes of various land use types over historical periods, especially the last 100 years, has become a hot research topic [13]. The field of economics also uses data on the size of ancient cities, the area of regional urban systems in particular, as an important modeling instrumental variable [14].

In recent years, several sets of historical land use datasets have been established at varying scales by related scholars, such as the Global Land Use Dataset from the University of Wisconsin [15,16], the Global Historical Environmental Dataset from the Netherlands Environmental Institute [17,18], and the Chinese Traditional Agricultural District Cropland Dataset [19,20]. Many local records and historical archives have been preserved in China, and Liu et al. [21] reconstructed the area of cities in China in 1700 based on statistical documentary sources. However, previous studies have generally involved quantitative reconstructions, and the characteristics of the historical urban system have been less frequently investigated in terms of the spatial patterns. Reconstructing the characteristics of the urban system in the historical period also requires specific topographic map information for each city as a way to reconstruct the sizes of cities using geospatial attributes [22,23]. Such research is of great significance, as remotely sensed data can only be reconstructed for urban land during the past 40 years. Therefore, in order to reconstruct the structural characteristics of the Chinese urban system over the last 100 years and an urban area grid dataset with spatial attributes, we need to develop new methods and sources of materials.

With the excavation of a series of archives in recent years, large-scale military surveying and mapping topographic data conducted by the late Qing Dynasty and the Republic of China are considered a reliable data source for historical land use and reconstruction [24–26]. In addition, because cities have important strategic significance in military activities [27], such military topographic maps in urban areas have high measurement accuracy and utilize reliable data sources [28]. These topographic maps, largely completed in the 1910s and 1930s, have clear city wall boundaries and can therefore be used to reconstruct the area of the city in the historical period (Figure 1). Chinese society in the middle of the Republic of China (1930s) was still in the traditional agricultural era, so this time period can be regarded as the traditional Chinese era (TCE). This collection of maps covers mainland China, except for Taiwan province, where information is temporarily missing. Therefore, the temporal and spatial scopes of this study were defined as cities at or above the county level in mainland China during the TCE (1930s). The main objectives of this study were as follows. First, using historical military topographic maps and GIS-based modeling, the extent of the city walls of each city was extracted and the area of the city was calculated. Second, the structure and characteristics of the urban system in the TCE were identified according to the administrative area division using methods such as the fractal and rank-size law. Third, a $1° \times 1°$ grid dataset with spatial attributes for the scale of urban land use in the TCE was generated.
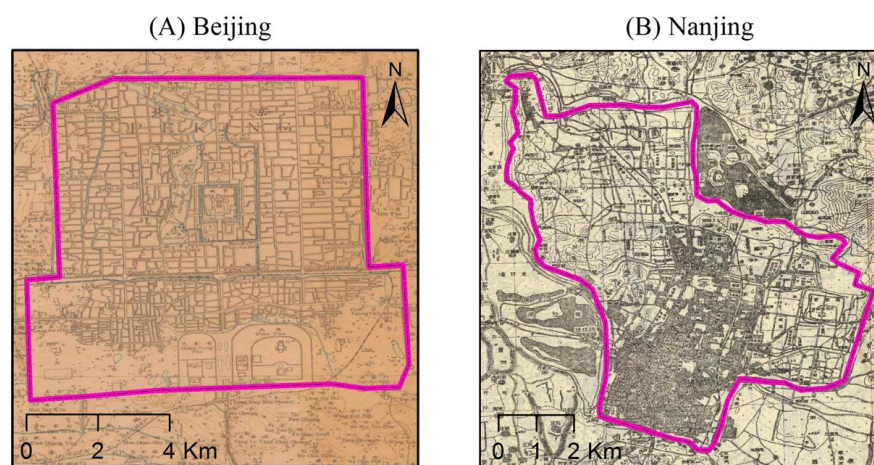
(A) Beijing (B) Nanjing

Figure 1. *Cont.*
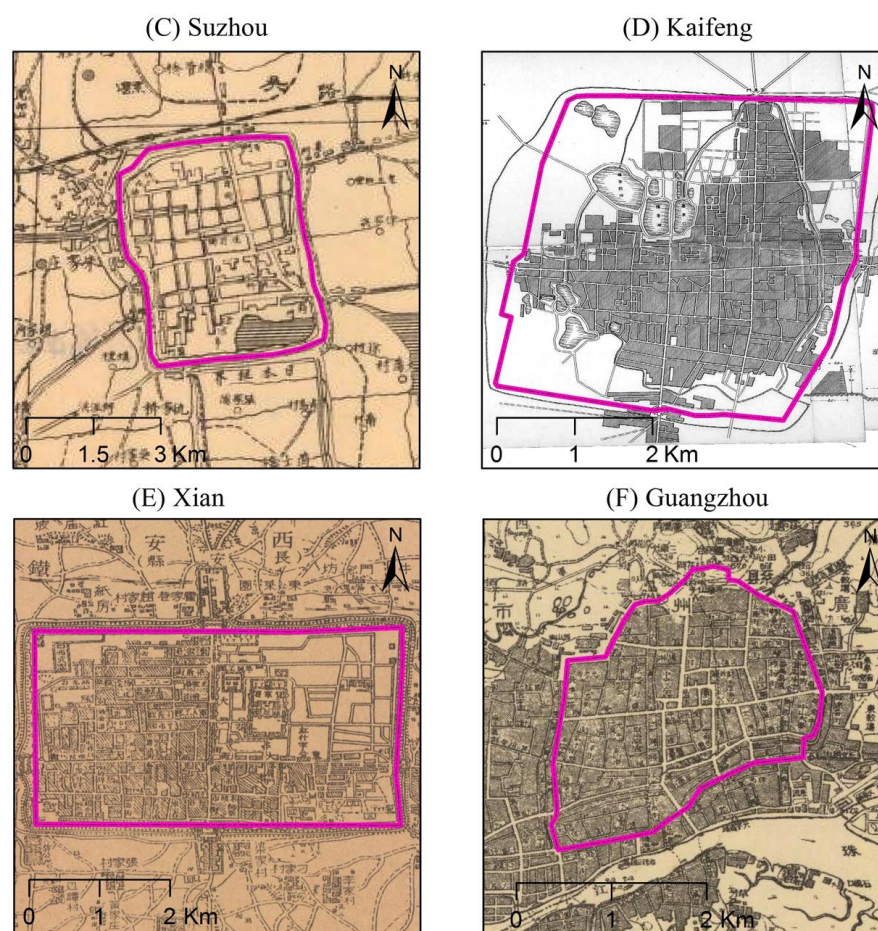
Figure 1. Example of the urban scope marks in the military topography of the Republic of China (**A**–**F** represent Beijing, Nanjing, Suzhou, Kaifeng, Xian, and Guangzhou, respectively).

2. Research Area, Data, and Methods

2.1. Definition of the Scope of the Research Area

Considering the possibility of obtaining data and facilitating comparative study, land use reconstruction in historical periods is still based on the modern administrative scope [29,30]. The Chinese Modern Administrative Region can be roughly divided into regions such as the Central Plains, the southwest, South China, Jiangnan, the northwest, and Northeast China. Among these, the measured work of the topographic maps in the Central Plains, Jiangnan, and South China began during the late Qing Dynasty; hence, the information was relatively sufficient. The surveying and mapping work in related cities and regions in the northeast and northwest regions were also conducted as part of the work during the Republic of China. Due to the high altitudes in Tibet, which may lead to difficult conditions for human habitation and the development of urban systems, from the perspective of measured map data from the 1930s, there was a lack of a clear urban scope (Figure 2).

To better connect the statistics of the current administrative division's data statistics and the comparative analysis of long-term sequence land use data, the provincial administrative unit of this study utilized the administrative division of 2020. In addition, due to the actual conditions when the statistics were conducted, Hebei included Beijing, Tianjin; Su-Hu included Jiangsu and Shanghai; Gan-Ning included Gansu, Ningxia; and Chuang-Yu included Sichuan and Chongqing, with a total of 27 units of analysis. The placement of the administrative borders utilized the China Historical Geographic Information System (CHGIS) dataset (http://fas.harvard.edu/~chgis, accessed on 12 June 2022) jointly developed by Harvard University and Fudan University. In terms of the selection of the grid

network specifications, the reconstruction of the grid network was based on $1° \times 1°$. In the mid-latitude region of China ($40°$ N), this grid covers an area of about 9454.61 km^2.

1 Heilongjiang	7 Shandong	13 Jiangxi	19 Yunnan	25 Inner Mongolia
2 Jilin	8 Anhui	14 Fujian	20 Chuan-Yu	26 Tibet
3 Liaoning	9 Su-Hu	15 Guangdong	21 Shaanxi	
4 Jing-Jin-Ji	10 Zhejiang	16 Hainan	22 Gan-Ning	
5 Henan	11 Hubei	17 Guangxi	23 Qinghai	
6 Shanxi	12 Hunan	18 Guizhou	24 Xinjiang	
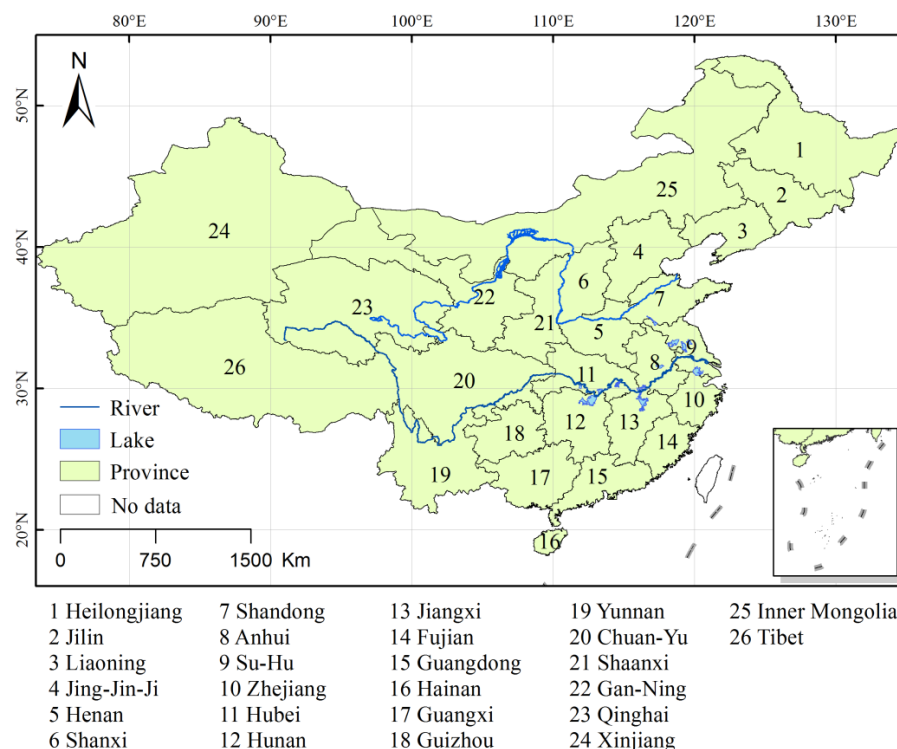
Figure 2. The geographical scope of the research area.

2.2. Military Topographic Map Information

The 1:50,000 military topographic maps of the Republic of China used in this study were derived from the national basic military topographic mapping plan of the General Staff of the Ministry of National Defense at that time. The mapping and cartography were concentrated in the 1910s and 1930s. These military topographic maps were used for military purposes at that time, so the accuracy of mapping was high, especially in urban areas. This collection of topographic maps basically covers most of China [26,31], except for nonurban areas in Qinghai, Xinjiang, Inner Mongolia, and Tibet. The map collection was obtained from the Institute of Modern History, Academia Sinica (http://map.rchss.sinica.edu.tw/, accessed on 13 June 2022) [32]. Some maps of eastern China, including Heilongjiang, Jilin, Liaoning, and Jing-Jin-Ji, were also supplemented by the Sino-American Cooperative Aerial Survey Team during World War II, the University of Texas Library, USA (https://maps.lib.utexas.edu/maps/ams/china/, accessed on 13 June 2022). The statistics indicate that the number of topographic maps in this collection is about 7300 [33]. The map size is 46 cm × 35 cm, and each map spans 15′ in longitude and 10′ in latitude (the space range is about 24.194 km by 18.532 km). The surveying and mapping method of the 1:50,000 military topographic maps utilizes triangulation, and the projection is the Lambert conformal conic projection [34]. This set of military topographic maps has a unique legend symbol for the walled part of the city, so the extent of the city can be derived from the topographic map based on the walls.

2.3. Ancient Chinese Administrative Divisions and Cities

Although the administrative divisions have changed frequently throughout China's history, since the Ming and Qing dynasties, the basic administrative divisions have been divided into three levels: provinces, prefectures, and counties. For administrative and military defense reasons, the seats of these administrative districts developed into provincial, prefectural, and county cities. This pattern of administrative divisions and urban

development was inherited by the later Republic of China and has continued to influence the pattern of urban systems in modern China. From the late Qing dynasty to the Republic of China, the number of cities above the county level in China remained relatively stable at about 1500 [35]. These cities above the county level form the basis of the current Chinese urban system, which contains about 1700 cities above the county level. Considering that many new county-level administrative units were established after the founding of the People's Republic of China, it can be assumed that county-level cities have a strong historical resilience in the structure of China's urban system. Therefore, the criteria adopted in this study for selecting the surveyed number of cities was that all of the cities in the area covered by this set of military topographic maps were counted.

2.4. Walled Cities in China

Although the construction of walled cities began early in China's history, the walls of these cities have been maintained and repaired throughout the subsequent phases of history [36]. After extensive construction of city walls during the Ming and Qing dynasties (1368–1911), most cities above the county level in China had city walls [37]. With the widespread use of military weapons such as artillery and the gradual modernization of China, the defensive function of the city walls gradually disappeared. Beginning in the 1940s, the development of many Chinese cities began to expand beyond the limits of the city walls. The walls of most Chinese cities were also demolished during this process [38]. Considering that this study focused on reconstructing the size and systemic structure of cities in the 1930s, the specific time of the construction of each city did not affect the results of the study. Due to changes in administrative divisions throughout China's history, the number of cities above the county level has changed from dynasty to dynasty. In this study, a total of 1265 cities at or above the county level were reconstructed based on military topographic maps.

Although some cities in the Chinese traditional period had built-up areas beyond the city walls [39], we chose the city walls, an intuitive criterion, as the basis for determining the city's extent, because this study focused on the characteristics of the urban system in the TCE as a whole. The extent of the city walls is the most direct symbol of ancient Chinese cities. It has been shown that although not all of the area within the city walls was utilized during the TCE, and some areas outside the walls may have been built-up urban areas, the percentages of these phenomena were not significant. Therefore, related studies have generally offset these occurrences against each other and have considered the city wall area to be the urban extent during the historical period [23].

2.5. GIS Reconstruction

2.5.1. Reconstruction Process

Relevant military topographic maps has information such as latitudes and longitudes, and we utilized the ArcGIS 10.2 (ESRI Inc., Redlands, CA, USA) for spatial georeferencing (this process can utilize other GIS software, such as the open source QGIS and not just ArcGIS software). The process of georeferencing historical topographic maps consists of three main steps. First, the 1:50,000 index diagram of each province was spatially aligned to the boundaries using the georeferencing tool in GIS software. In this way, preliminary alignment is obtained for each 1:50,000 topographic map. Second, the 1:250,000 Sino-American Cooperative Aerial Survey Team topographic map was then spatially aligned to its own latitude and longitude on every map four corners. Because the area covered by these 1:250,000 maps is not large, it is about equal to the extent of 160 km by 110 km. After controlling the longitude and latitude of the four corners of the map, the second order polynomial transformation provided by the georeferencing tool in ArcGIS software allows the whole map to obtain a better spatial projection effect. In the third step, the preliminary aligned 1:50,000 topographic map was compared with the 1:250,000 topographic map or remote sensing image according to the topographic features, such as mountain peaks, rivers, and other terrain features, to complete the fine-tuning. After completing the georeferencing

of the topographic map, the polygon tool in ArcGIS determined the city according to the city wall and the city area calculated using the geometry tool. Finally, the scale of urban land was calculated in the $1° × 1°$ grid. The detailed GIS reconstruction workflow is shown in Figure 3.
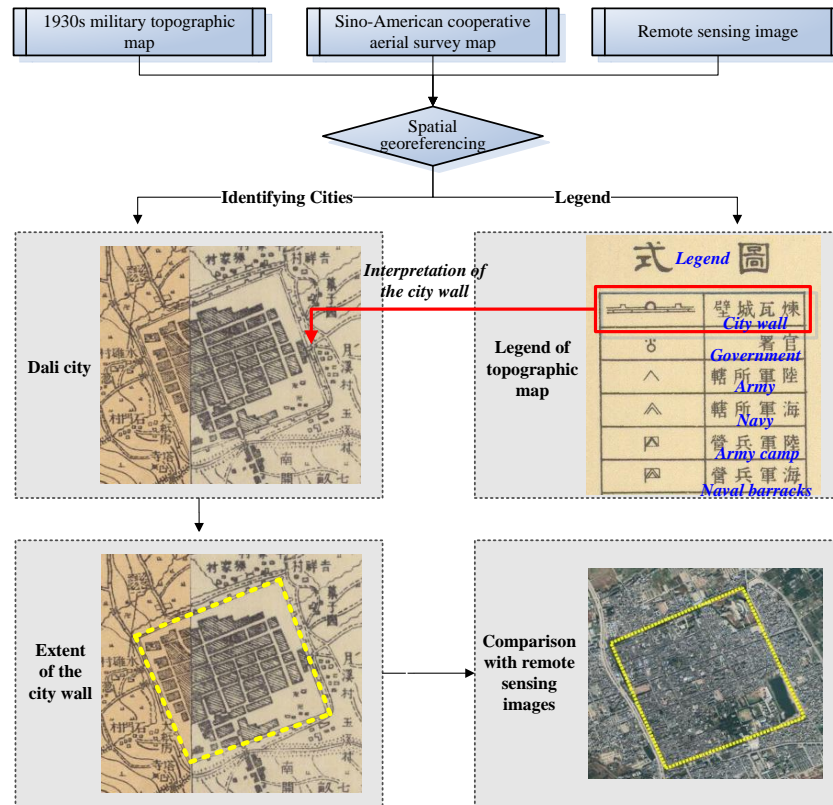
Figure 3. GIS reconstruction workflow on city extent in TCE.

2.5.2. Accuracy Evaluation

The accuracy of the reconstruction results was compared and analyzed using cities that are still preserved and still have relatively complete city walls. The specific method was to sort out and collect China's currently preserved city wall remote sensing images. Based on Google Earth, the city wall lengths and urban scales were measured to evaluate the accuracy of this reconstruction result.

2.6. Fractal and Rank-Size Law

The size distribution of the urban system has the characteristics of self-similarity and is fractal [40]. Hence, the fractal model was used to calculate its fractal dimension. In a specific area, the urban rank and the city size are in agreement with the order of the rank-size rule, and the expression is

$$S_i = S_0 × Ri^{-q} \tag{1}$$

where Si in the equation is the size of the i-city; S_0 is the theoretical value of the first city size; Ri is the first city rank; the q is the Zipf dimensions. Generally, the upper equation can be utilized to calculate the logarithm and obtain the following:

$$\ln S_i = \ln S_0 - q \ln R_i \tag{2}$$

where the least squares method is utilized to obtain the fractal dimension, q. Studies have shown that [41,42], when $q > 1$, the cities in the area are more concentrated, and large cities are prominent; when $q < 1$, the cities in the area are scattered, and small or medium-size

cities are more developed. Theoretically, the relationship between q and D depends on the fitting coefficient of the equation [43]. The empirical equation shows that q and D are reciprocal to each other in the case where the fitting coefficient of the equation is close to 1, that is:

$$q \times D = 1 \tag{3}$$

Through this formula, the fractal dimension D of the urban system can be obtained. The change in fractal dimension D can reflect the balance of the urban system. The larger the balance, the closer the scale between cities, the smaller the gap between each other, the more balanced the city, and the lower the urban primacy index. On the contrary, the more uneven the size of the city system, the higher the urban primacy index. Related studies have shown that $\ln S_0$ represents the structural capacity of the urban system. The more complicated the urban system, the larger the overall scale, the larger the structural capacity; on the contrary, in the simple urban system, the overall size is smaller, and has a smaller structural capacity.

2.7. Coefficient of the Variation and the Urban Primacy Index

The coefficient of variation (CV) can eliminate the difference between the size of a single city and obtain the change degree of the whole city. CV is used to measure the degree of difference between the size of each city in a region, and its calculation method is the ratio of the standard deviation of the scale value of all cities in the region to the average value. The urban primacy index is a common method for describing and analyzing the structure of city systems and consists primarily of the 2-city index (K_2), the 4-city index (K_4), and the 11-city index (K_{11}) [43,44]. In addition, to reflect the status of the first city in the urban system, K_1 was defined as the first urban primacy index, that is, the first city in the region accounted for the proportion of all cities in the region. The calculation method is:

$$\begin{cases} K_1 = S_1 / \sum_{i=1}^{i} S_i \\ K_2 = S_1 / S_2 \\ K_4 = S_1 / \sum_{i=2}^{4} S_i \\ K_{11} = 2S_1 / \sum_{i=2}^{11} S_i \end{cases} \tag{4}$$

In the formula, K indicates the urban primacy index, S_i is the size of the i city.

2.8. Space Lorentz Curve

Economist M. Lorrenz put forward the space Lorentz curve method [45,46] in the process of studying the balance of economic development, and it was later used by many disciplines for research on differential patterns. For study on the concentration and balance of spatial data, the Lorenz curve is an important method. Lorenz curve can reflect space concentration of urban system. If the curve is closer to the absolute uniform line, the distribution of the scale of the urban system in the region is more uniform; otherwise, the distribution is more concentrated.

2.9. Getis–Ord Cold and Hotspot Analysis

Getis–Ord statistics allow us to identify areas that are statistically spatially hot versus cold. It can help us to identify areas with higher index values or lower index values in and around the region. Therefore, it is also called cold- and hotspot analysis. Cold- and hotspot analysis can help us more accurately identify the spatial gathering of a certain element in the area [47,48]. Therefore, the agglomeration or decentralization of urban land in the area in the area can be identified by Getis–Ord G_i^*. The relevant formulas are:

$$G_i^* = \frac{\sum_j w_{ij} x_j - \overline{x} \sum_j w_{ij}}{S \sqrt{\frac{[n \sum_j w_{ij}^2 - (\sum_j w_{ij})^2]}{n-1}}} \tag{5}$$

In the formula, n is the total number of samples, $\bar{x}$ is the average value, w_{ij} is a spatial weight matrix, and S is the standard deviation. In general, G_i^* will be normalized:

$$Z(G_i^*) = \frac{G_i^* - E(G_i^*)}{\sqrt{Var(G_i^*)}} \tag{6}$$

In the formula, $E(G_i^*)$ is the expected value, and $Var(G_i^*)$ is the variance.

3. Results

3.1. Urban Area Reconstruction

In this study, the extents of a total of 1265 cities at or above the county level in the middle of the Republic of China (1930s) were calculated (Figure 4) that were distributed in 25 provincial-level administrative regions in the country. Among these, there were 25 cities at or above the provincial level, 179 cities at the prefecture level, and 1061 county-level cities. Among these, the largest city was Beijing, with an area of 58.5 km². The smallest city in the region was Xinjiang Jinghe, with an area of 0.02 km². The average value of all cities above the county level was 1.10 km², and the standard deviation was 2.37 km².
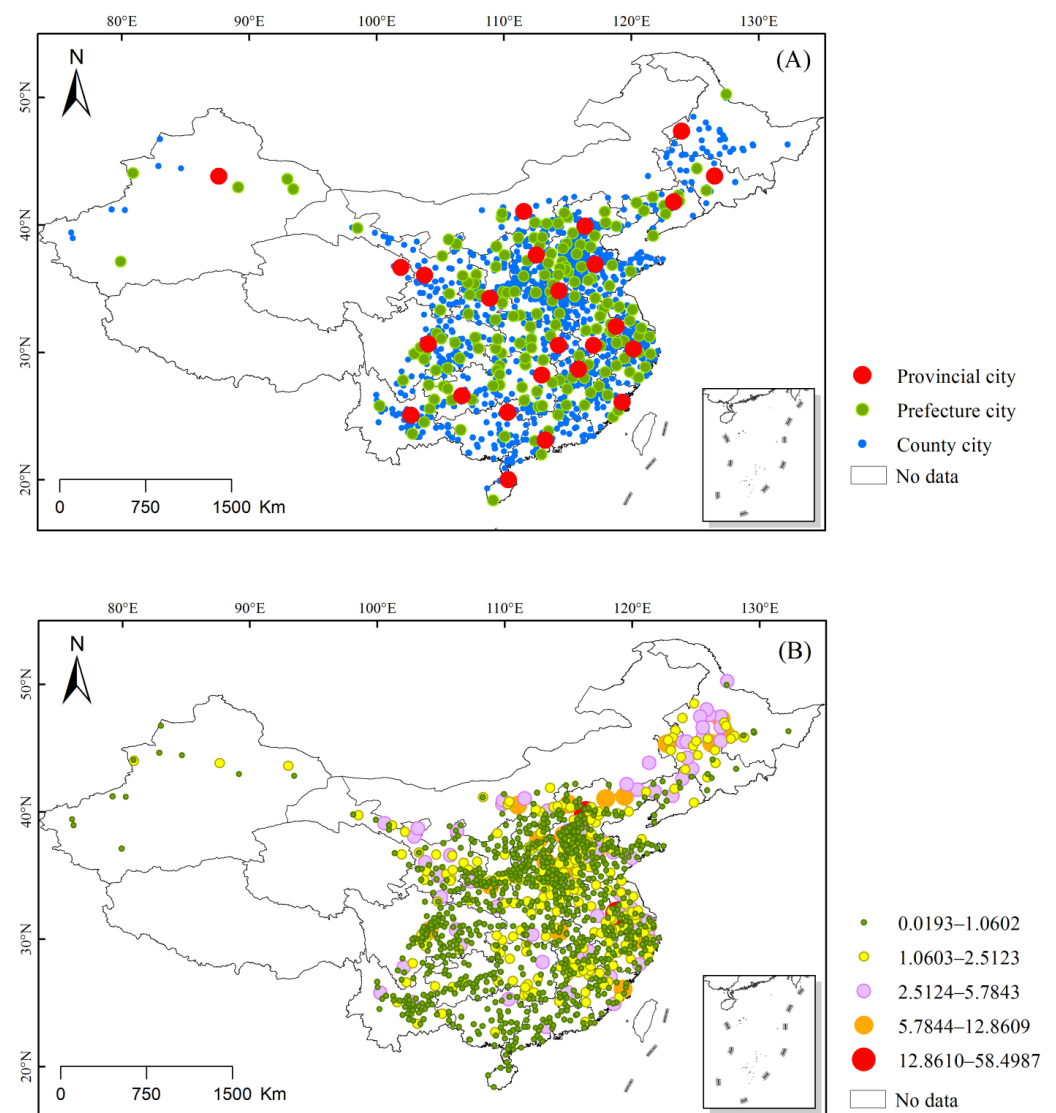
Figure 4. (**A**) Distribution of urban areas at or above the county level and (**B**) urban areas in the TCE. The data were classified using the Jenks natural breaks method.

3.2. Level of Urbanization of the Grid

Based on the reconstruction method discussed in Section 2.5, a gridded reconstruction of the land scale of cities at or above the county level in China during the traditional period was conducted to obtain a $1° \times 1°$ resolution urban land scale dataset (Figure 5). Of the total 1096 grids, 710 had an urban area of 0. The remaining 386 grids had a maximum value of 62.93 km^2 and a minimum value of 0.02 km^2. Figure 4 shows the distribution of the city sizes in China during the traditional period, which was characterized by high levels in the north, low levels in the south, high levels in the east, and low levels in the west of the country, and this was also associated with flat topography and more developed agriculture of the North China Plain and the Central Plains of China providing the ability to support larger cities. In contrast, against the background of lower urban sizes in the west and south, the larger urban sizes in regions, such as the Chengdu Plain and the Pearl River Delta, were clearly associated with topography and more developed agriculture and commerce. In addition, the spatial distribution of city sizes within each province was generally consistent with the urban hierarchy, with the provincial or prefecture cities generally being located in a grid of larger cities. As can be seen from Figure 5, the regional grid city size values for western Sichuan, western Yunnan, Qinghai, Xinjiang, and Tibet were zero. These areas are generally ethnic minority concentrations, and their production structures and levels of agricultural development differ significantly from those in the east. In addition, their urban development is relatively backward.
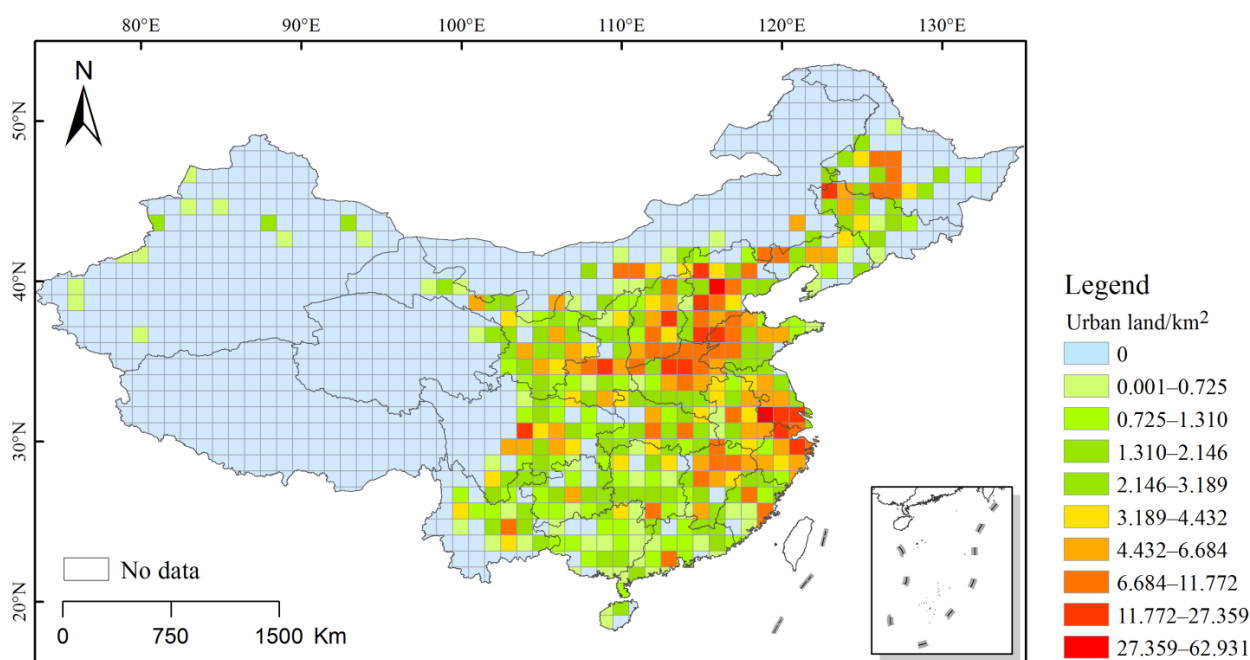
Figure 5. Reconstruction of the urban scale grid in the TCE.

3.3. Urban System Structure

There were a total of 1265 cities above the county level within the study area, and the total land size of all the cities was 1396.48 km^2, with a mean value of 1.10 km^2 and a coefficient of variation (CV) of 2.15. As a whole, all cities as a system of cities had urban primacy indexes of $K_1 = 0.041$, $K_2 = 1.397$, $K_4 = 0.868$, and $K_{11} = 0.841$. The rank-size curve (Figure 6A) and the double-logarithm scatter plot (Figure 6B) showed that the urban system in traditional China was one in which large cities were not significantly developed ($q = 0.83 < 1$, $R^2 = 0.91$), and the proportion of small cities, which were generally county-level cities, was high. As can be seen from Figure 6A, except for the first two cities with large area, the other cities have little change in area with the increase in location sequence. For the urban system in this period, most cities were small cities. This characteristic of the

urban system was also related to the fact that during the Republican period, China was still a traditional agricultural country, with cities being more administratively dominated and commercial cities not yet developed.
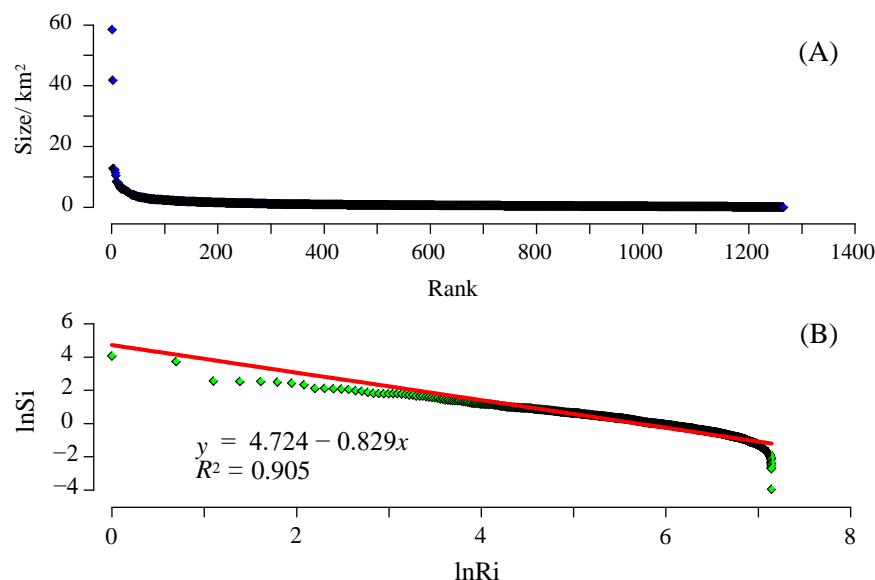
Figure 6. City rank-size curve (**A**) and double logarithmic scatter plot (**B**) of the rank-size distribution in the TCE.

The urban system characteristics of the provinces were measured using the coefficient of variation (CV), the city primacy index, and the fractal dimension. The results showed (Figure 7) that the urban system characteristics varied significantly between provinces and regions. The coefficients of variation were larger in the provinces of Jing-Jin-Ji, Su-Hu, and Chuan-Yu, which also indicated that there were significant differences in city sizes within these provinces and regions, with large cities and small cities existing at the same time. Although the urban system in the TCE has certain common characteristics, the study of urban system in different regions also shows that the development of urban system in different regions has different characteristics. This also suggests that we need to consider the differences in the development of different regions when studying the urbanization of China in the historical period. This led to their larger coefficients of variation. In terms of the urban primacy index, all indicators were larger in Jing-Jin-Ji and Su-Hu, indicating that there were more pronounced urban primacy index effects in these two regions. This result also agreed with the role of Beijing and Nanjing, the two largest cities in the urban system of their provinces. The R^2 of the double logarithm of the city rank-size fit for the 25 provinces and regions was nearly greater than 0.7, which was a good fit and indicated that their city size distribution had fractal characteristics; for example, small cities constitute the majority of the urban system. The fractal dimension of most provinces was near 0.8 to 0.9, for which it is generally considered that when $q < 1$, the distribution of urban sizes in the region is more dispersed, and small and medium-sized cities are more developed. Only the provinces of Su-Hu, the northeast, and the frontier regions had fractal dimensions of $q > 1$, which also indicated that the Su-Hu region had developed to the stage of city primacy during the traditional Chinese period. The reason for a fractal dimension of $q > 1$ in the northeastern and frontier regions other than Su-Hu was primarily due to the underdevelopment of cities in these regions, the small number of cities, and the absolute dominance of some provincial cities in terms of city size within the province due to military or other reasons.
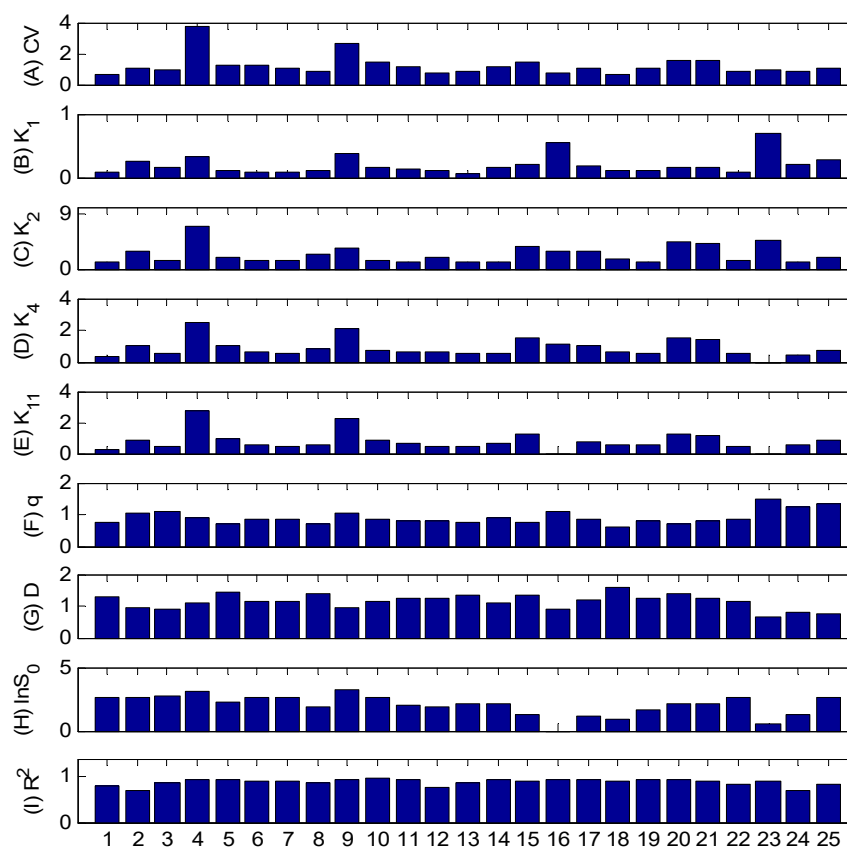
Figure 7. Index of the primary characteristics of the provincial urban system in China during the TCE (CV: coefficient of variation; K1, K2, K4, K11: urban primacy index; *q*: Zipf dimensions; D: fractal dimension; $\ln S_0$: logarithm of theoretical value of the first city size; R^2: determination coefficient of rank size equation).

3.4. Spatial Clustering Characteristics

The results of the Lorenz curve calculation are shown in Figure 8. The cumulative frequency curve of the rank size of cities above the county level in China during the traditional period has a downward concave form. As the curve lies below the line of uniform distribution (i.e., the diagonal line in the diagram), it can be concluded that the distribution of cities during this period was in a state of agglomeration with nonuniform spatial distribution. It is difficult to quantitatively describe and analyze the distribution of urban system in TCE. This study obtains the spatial Lorentz curve of urban system through the restoration of cities one by one in the topographic map, which has important reference significance for future research. By calculating the degree of concentration of the curve, i.e., the ratio of the area under the cumulative frequency curve to the area under the uniform distribution line, a value of 0.50 was derived for the degree of concentration. This shows that the distribution of urban system in TCE is between uniform distribution and extreme distribution. The most extreme situation is that all urban areas are concentrated in one big city, which is only the most extreme situation in theory.

3.5. Spatial Trends

The spatial trend analysis showed that there was a north–south and east–west trend in the size of Chinese cities above the county level during the traditional period in terms of large-scale spatial patterns (Figure 9). In general, the distribution of city sizes tended to increase from west to east and decreased from north to south. This pattern of the spatial distribution was also consistent with the results of the map analysis shown in Figure 4B. The primary reason for this pattern is that the eastern portion of China had been ahead

of the western region in terms of urban development during the traditional period. In contrast, the north, with its long history of development and more plains, had also seen a larger scale of urban construction than the south.
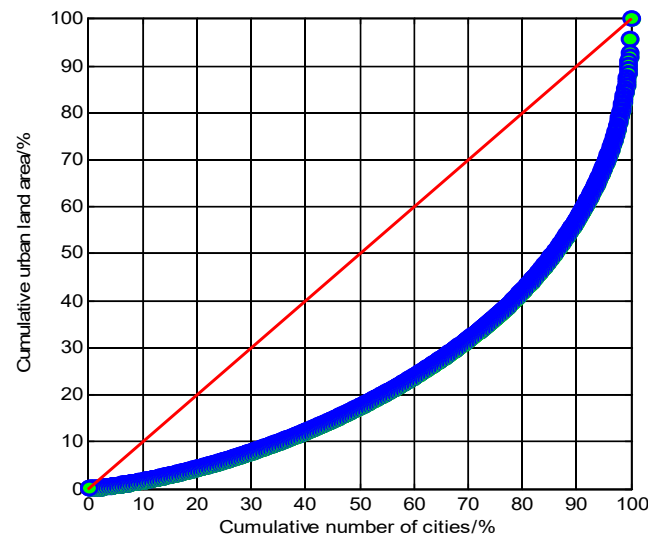
Figure 8. Lorenz curve of the distribution of urban systems in China during the TCE (The red line represents the uniform distribution of cities in the urban system. The blue dot represents the cumulative number of cities and cumulative urban land area in TCE).
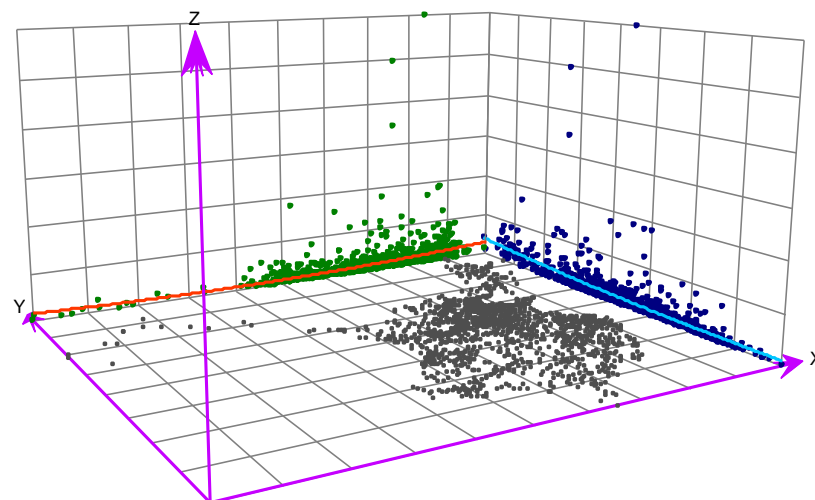
Figure 9. Spatial distribution trends of cities in China during the TCE.

To further analyze the different spatial patterns of cities above the county level across the country during the traditional period, all cities in the study area were analyzed in groups at 10° intervals in the longitudinal direction and 5° intervals in the latitudinal direction. The results of the kernel density and frequency analyses showed that in longitude, China's traditional period cities at the county level and above were primarily distributed between 100° E and 130° E (Figure 10A), while in latitude, most cities were distributed between 20° N and 50° N (Figure 10B). The kernel density curve of the distribution showed that the cities were more evenly distributed at latitude, closer to a normal distribution. This shows that the distribution of cities in TCE is more balanced in the north–south direction. A large number of cities are concentrated in the mid latitude area, and there are relatively few cities very close to the north and south frontier region. At longitude, the distribution was skewed towards a concentration between 110° E and 120° E. The results of the box plot analysis of the size distribution of cities above the county level in each group showed that

the mean city size tended to increase gradually in both longitude (Figure 10C) and latitude (Figure 10D), and the dispersion within the group also tended to increase with increasing longitude and latitude. In terms of longitude distribution, there are relatively few cities in western China. This is also related to the small population in western China. The cities in Northeast China are relatively large. The reason for this phenomenon may be that the terrain in Northeast China is relatively flat and suitable for urban development.
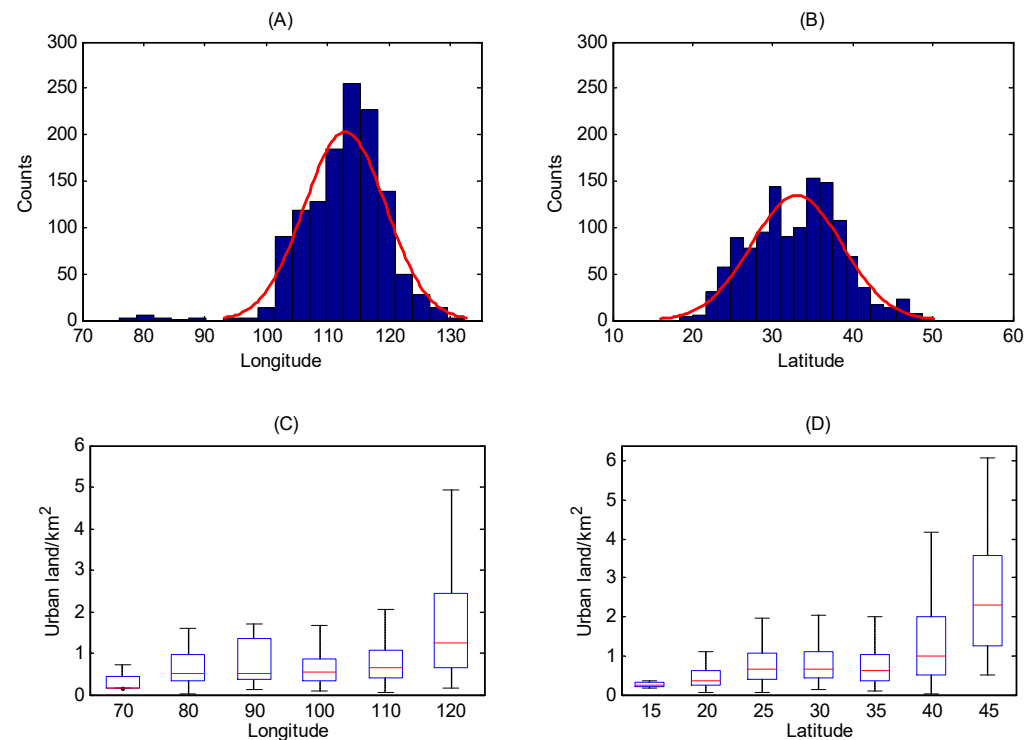
Figure 10. Kernel density maps of the spatial distribution (**A**,**B**) and size distribution box plot (**C**,**D**) of cities in China during the TCE.

3.6. Characteristics of the Regional Agglomeration of Urbanization Levels

The results of this urban scale grid reconstruction (Figure 5) showed that certain urban agglomerations with high levels of urbanization were already formed in China during the traditional era. For example, Jing-Jin-Ji, Henan, Shandong, and other central plains; Su-Hu, Anhui, Zhejiang, and other southern regions. There were also city clusters of certain sizes in the Chengdu Plain, the Pearl River Delta, and the Guanzhong Plain. The results of the Moran analysis showed a z-score of 12.81 ($p < 0.001$) (Figure 11). This result suggested that the spatial distribution of city sizes above the county level in China during the traditional period was characterized by extreme clustering. This meant that areas with high city size values were also surrounded by high value areas, and areas with low city size values were surrounded by low value areas.

GIS software was used to classify the number of cities above the county level in China during the traditional period according to the provincial administrative regions to which they belonged (Figure 12), the results showed that Shanxi, Henan, and Zhejiang had the highest urban densities of 6.70, 6.26, and 6.09 cities/10^4 km^2, respectively. Provincial administrative regions with relatively low urban densities included Inner Mongolia, Xinjiang, Qinghai, and Tibet. A kernel density analysis of the urban density showed a contiguous area of highly concentrated urban density forms in the regions of the North China Plain, Shanxi, and the Guanzhong Plain in northern China, and these were also the primary urban agglomeration areas in China during the traditional period. In addition, small areas of high urban density formed in the Yangtze River Delta and the Chengdu Plain.
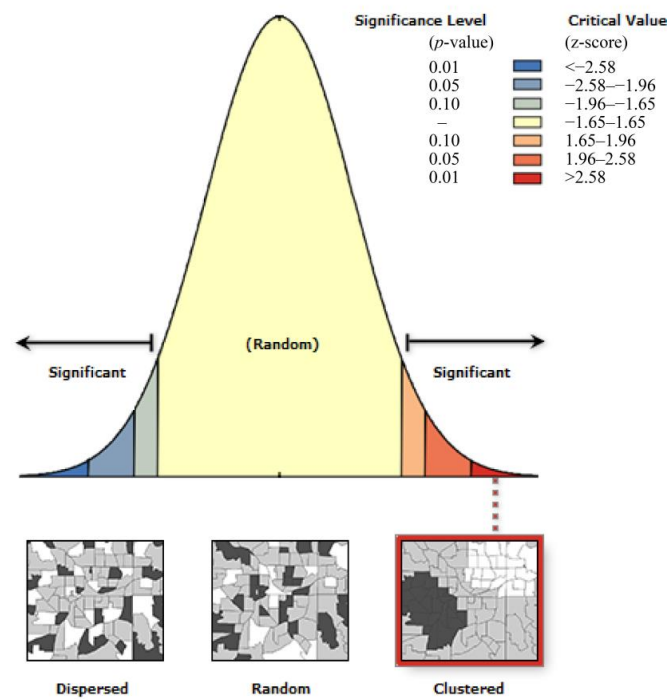
Figure 11. Moran analysis of the spatial agglomeration of urban systems in China during the TCE.
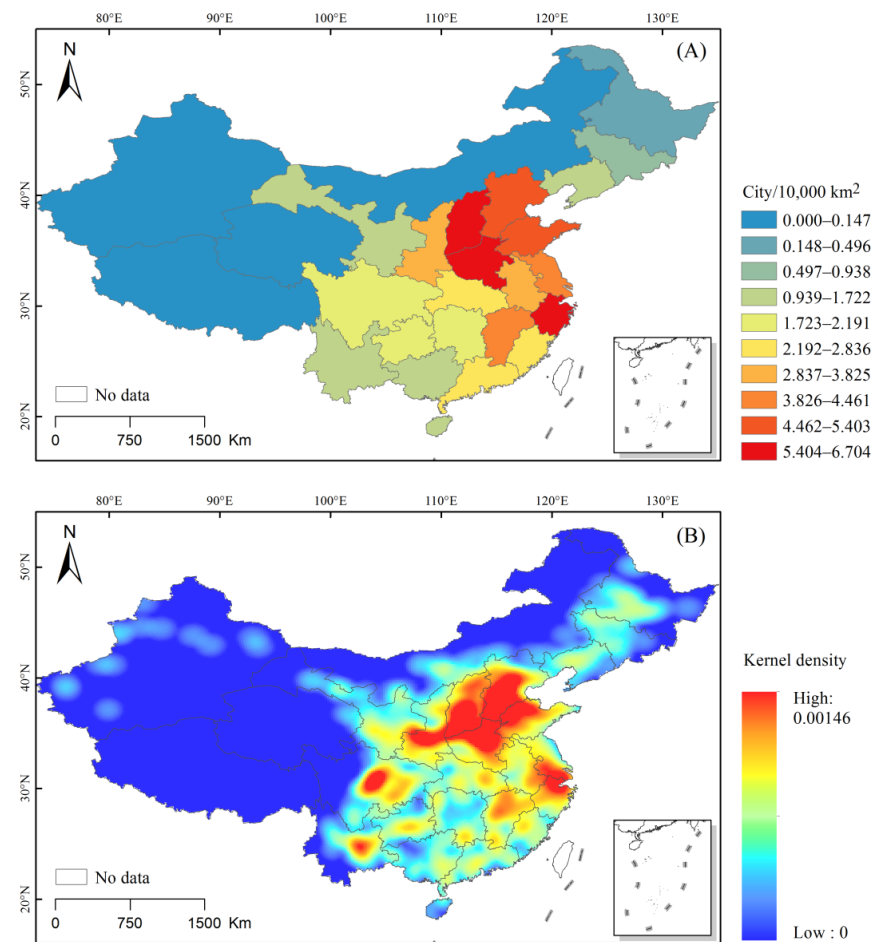
Figure 12. Density of the number of cities by province (**A**) and the kernel density analysis (**B**) in China during the TCE.

To better reflect the spatial distribution characteristics of urban agglomerations, the reconstructed urban land scale grid dataset was analyzed using the hotspot analysis function in the GIS model, and the results are shown in Figure 13. A hotspot analysis of the urban scale of the $1° \times 1°$ grid during the Republic of China period revealed three primary agglomerations, namely the Jing-Jin-Ji region, the border area between northern Henan and Shandong, and the Yangtze River Delta.
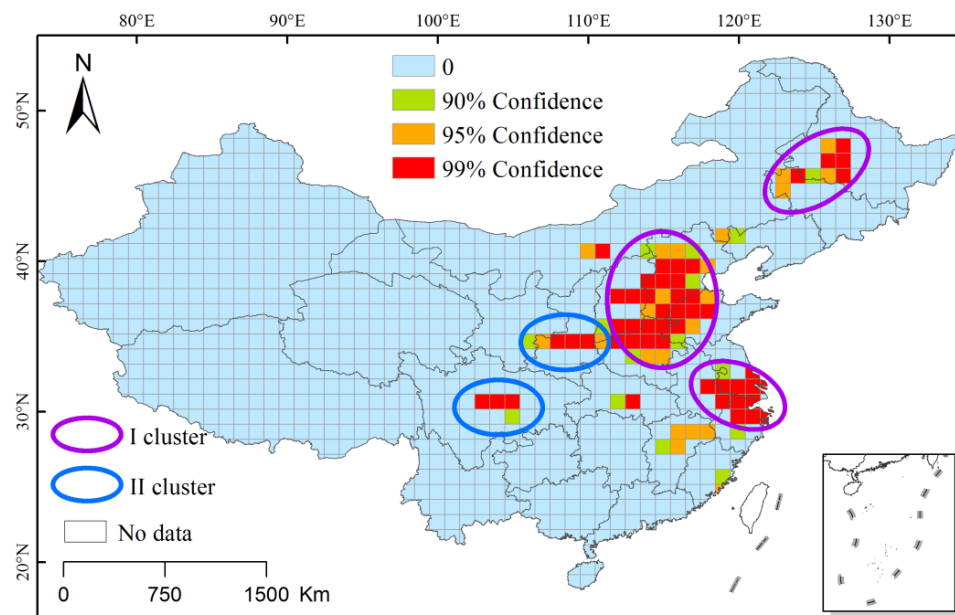
Figure 13. Hotspot analysis of the grid level of urbanization in the TCE. (The red area indicates the hot spot area that passed the 99% confidence test; the yellow area indicates the hot spot area that has passed the 95% confidence test; the green area indicates the hot spot area that has passed the 90% confidence test. The purple circle indicates the hot spots cluster region; the blue circle indicates two secondary hot spots cluster region.)

3.7. Differences in Urban Systems at the Provincial Level

Although, overall, all cities at or above the county level constitute an urban system with a fractal dimension of $q < 1$ and are of the type where smaller cities are more developed and larger cities are less pronounced, this does not mean that all provinces and regions are of this type. To compare the variability in the distribution of city size between provinces and regions, a scatter plot of the combined use of the urban primacy index (K_2) and the total urban land area proposed by Xu et al. [49] was used to illustrate the inter-provincial differences in city sizes. As shown in Figure 14A, as the total size of the urban land in the province and region increased, their urban primacy index was also higher. There was a significant positive correlation between the urban land and the urban primacy index (K_2), with a correlation coefficient of 0.362, $p < 0.01$. Among these, Jing-Jin-Ji and Su-Hu had a large total urban land size and a high urban primacy index, while Xinjiang and other provinces and regions had small total urban land sizes and insignificant first city development. The results shown in Figure 14B indicate that the total size of urban land in the province shows a degree of positive correlation with the average size of individual cities within the province, with a correlation coefficient of 0.35, $p < 0.01$. Although the Jing-Jin-Ji region had the largest total urban area, the differences between cities were more pronounced, with smaller gaps between cities in the Su-Hu region and larger average city size.
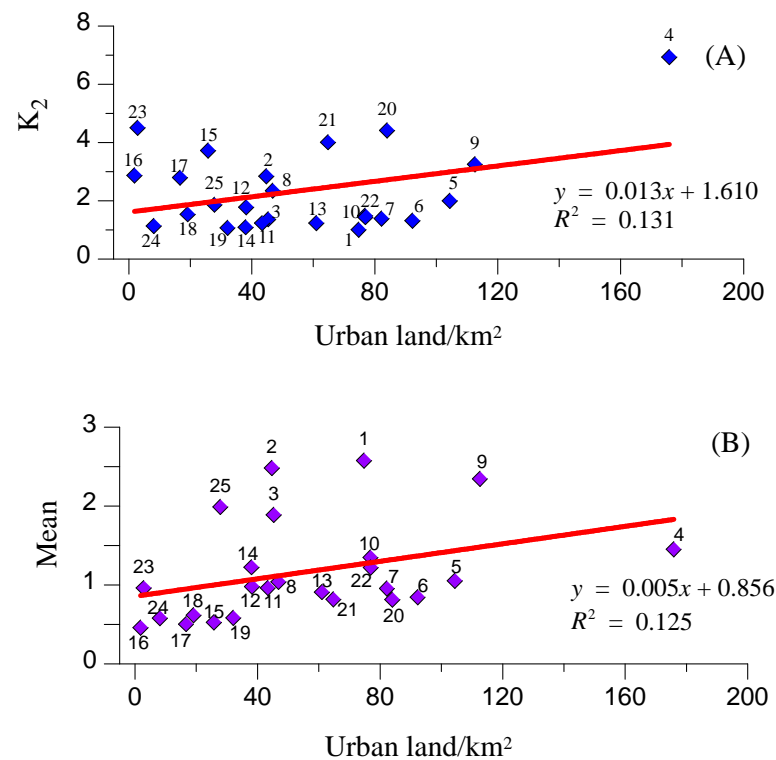
Figure 14. Scatter plot of the interprovincial differences in urban land use with K_2 (**A**) and mean land scale (**B**).

4. Discussion

4.1. Comparison with Other Urban Land Use Data

Previous studies have been limited by the materials available and have less frequently examined the size of historic cities in China [32]. Using archival documents, He et al. [23] estimated the area of cities at or above county level in 18 provinces during the late Qing dynasty (1820s) based on a model and by assuming that all of the cities were square. By comparing the urban area data for the 1820s with the results of this study, a good correlation was found between the two datasets (Figure 15). The regression equation is $y = 1.6678x - 0.1212$ ($R^2 = 0.896$, $p < 0.001$). Since He et al. utilized a modeling approach rather than actual measurements, the results were overestimated by 66% overall. Further analysis yielded a Spearman rank correlation coefficient of 0.851 ($p < 0.001$) for the two datasets. Despite the numerical differences between the two data sets, the results of the regression analysis and the rank correlation coefficient test indicate that the results of this study are reasonable, and the differences may originate from the errors of the different reconstruction methods.

4.2. Types of Urban Scale Systems

To further discuss the types of urban size systems in each province of China during the traditional period, a cluster analysis was conducted for 25 provinces based on the coefficient of variation (CV), the urban primacy index (K_1, K_2, K_4, and K_{11}), the fractal dimension (q and D), the structural capacity ($\ln S_0$), and the coefficient of determination (R^2) of the regression equation for each province and region (Figure 16). The results showed that Jing-Jin-Ji and Su-Hu belonged to the first category. The urban system in this category was characterized by a high coefficient of variation and urban primacy index, a fractal dimension close to one, and a large structural capacity and $R^2 > 0.9$. The second category included Guangdong, Chuan-Yu, Shaanxi, Jilin, Hainan, Guangxi, and Qinghai. The urban system in this category was characterized by a medium range of coefficient of variation values, a high city primacy index, a small fractal dimension, medium structural capacity

values, and an R² of approximately 0.8. The remaining provinces and regions were divided into a third category, a group of urban systems characterized by a smaller coefficient of variation, a smaller degree of the urban primacy index, and a smaller structural capacity.
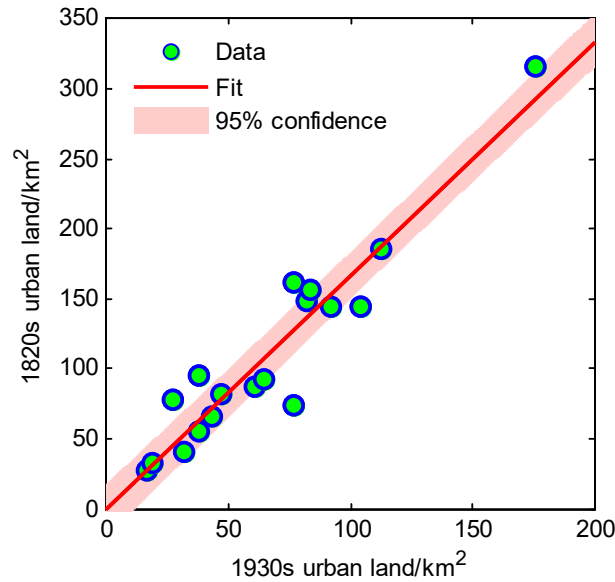
Figure 15. Scatter plot of 1930s urban land data and 1820s urban land data.
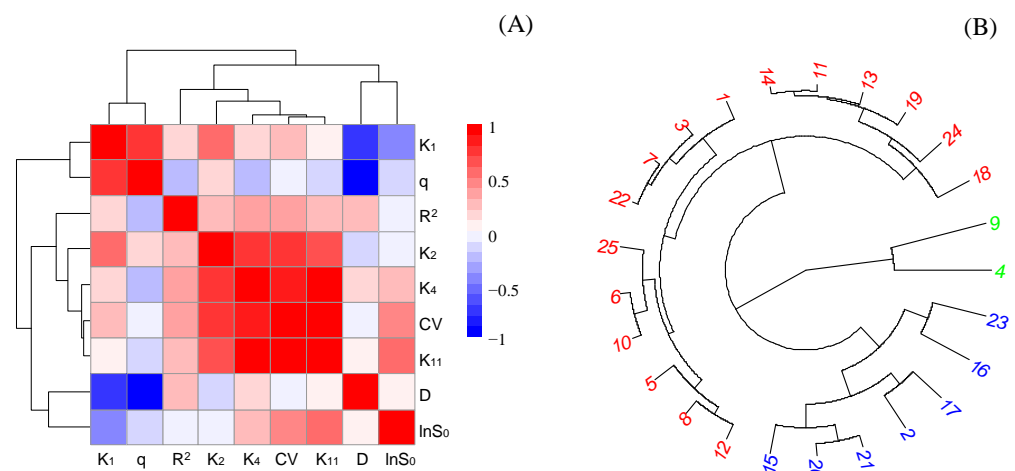
Figure 16. Heat map (**A**) and cluster map (**B**) of the urban systems in the TCE. The numbers 1–25 denote Heilongjiang, Jilin, Liaoning, Jing-Jin-Ji, Henan, Shanxi, Shandong, Anhui, Su-Hu, Zhejiang, Hubei, Hunan, Jiangxi, Fujian, Guangdong, Hainan, Guangxi, Guizhou, Yunnan, Chuan-Yu, Shaanxi, Gan-Ning, Qinghai, Xinjiang, and Inner Mongolia, respectively. The green, blue and red in the numbers 1–25 represent the three classification results.

4.3. Uncertainty Analysis: A Comparison Using Remote Sensing Data

The reconstruction of areas of ancient urban land may have certain errors. Therefore, to more effectively explain the reliability and error range of the reconstruction results, this study system sorted out the ancient cities in China that had relatively complete ancient city walls and utilized Google Earth's remote sensing image data to measure the area of the cities. In this manner, a set of verification data was obtained. The set of remote sensing survey datasets for ancient cities included 12 cities (Figure 17): Jingzhou, Zhengding, Heze, Qufu, Baoding, Datong, Xiangyang, Nanyang, Fenyang, Pingyao, Xingcheng, and Dali. The reasons for selecting these cities for comparative study were that (1) the ancient city walls of these cities have not been demolished and still remain within the modern cities;

(2) these cities were distributed throughout various regions of China as much as possible so that they are representative; and (3) suitable remote sensing image data were available and the city walls could be more obviously identified on the maps.
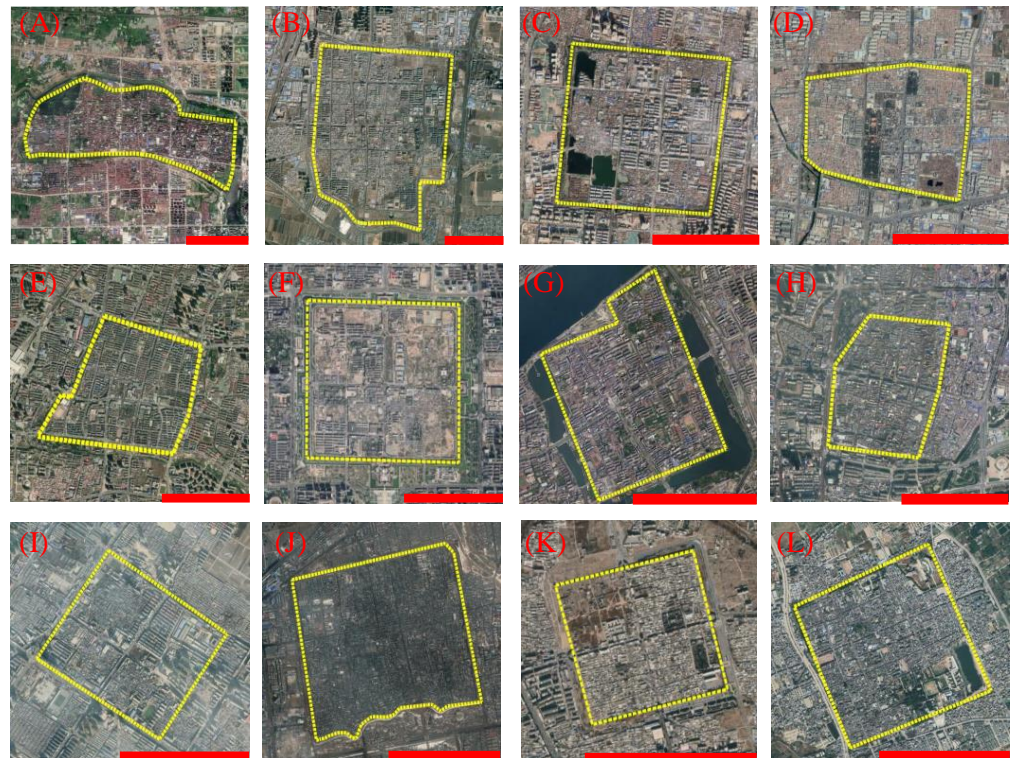
Figure 17. Google remote sensing image of a city in which the walls are still preserved (yellow lines indicate the extent of the wall. Letters (**A–L**) denote Jingzhou, Zhengding, Heze, Qufu, Baoding, Datong, Xiangyang, Nanyang, Fenyang, Pingyao, Xingcheng, and Dali, respectively. Scale bar = 1 km.

The walls of these cities are well preserved and could be interpreted from remote sensing images. The urban land areas of the cities based on the remote sensing image measurements were considered true values. Therefore, these results were obtained using a regression analysis of the historical data and remote sensing data. The correlation coefficient between the urban area reconstructed based on historical data and the remote sensing measurement data was 0.976, and the regression equation was $y = 0.944x + 0.106$ ($R^2 = 0.95$, $p < 0.001$). It can be seen that the reconstruction results are highly correlated with the remote sensing data (Figure 18).

4.4. Limitations

In addition to the uncertainty of the historical topographic maps in the reconstruction process, this study still has limitations in terms of the research methodology and research depth. Considering that the aim of this study was the reconstruction of urban systems, the analysis of individual cities in the historical period, as well as the point pattern of cities, needs to be strengthened. In this study, more common spatial analysis methods such as the spatial Lorenz curve, hot spot analysis, spatial trend analysis, and kernel density analysis were used. However, methods such as the mean center and standard deviation ellipse were not applied in this study because only the 1930s reconstruction data were available, which made it difficult to perform point pattern change analysis for different time periods. In the future, an attempt can be made to build a city size dataset for China during different time periods in the last hundred years and to conduct a complete spatial and temporal pattern analysis. In addition, since urban clustering studies require more indicators to describe cities, but at present, we are limited to historical data; we can only reconstruct the sizes of

cities in historical periods, so it is difficult to conduct urban clustering studies, which is also a limitation of our study.
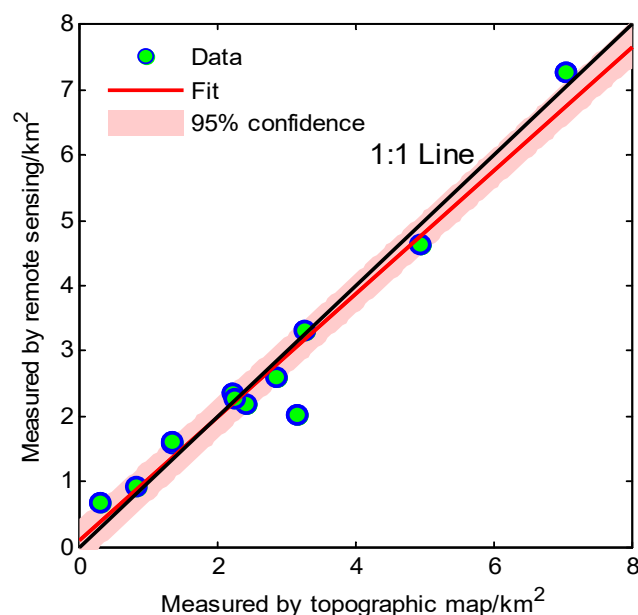
Figure 18. Scatter plot of the extent of the wall reconstructed from historical topographic maps, and the extent of the wall reconstructed from remote sensing imagery.

5. Conclusions

The structure of the urban system in the TCE (1930s) has not previously been studied quantitatively. This hinders the development of a database of urban land use in historical periods, especially gridded urban sites with spatial attributes. In this study, we attempted to measure the area of county level or above cities in mainland China using a GIS model and 1:50,000 military topographic maps from the 1930s. The following primary conclusions were drawn.

(1) A total of 1265 county level or above cities were counted in the TCE, including 25 provincial level or above cities, 179 prefectural level cities, and 1061 county level cities. Based on the extent of the city walls in TCE, the largest city was Beijing, with an area of 58.5 km^2, and the smallest city was Jinghe in Xinjiang, with an area of 0.02 km^2. The total land area of all of the cities was 1396.48 km^2, with a mean value of 1.1 km^2 and a standard deviation of 2.37 km^2.

(2) The results of the rank-size analysis indicate that the urban system in the TCE was characterized by large cities with insignificant development ($q = 0.829 < 1$, R$^2 = 0.905$) and a high proportion of county-level cities. The characteristics of this urban system were also related to the fact that in the 1930s, China was still a traditional agricultural country, the cities were more administrative-driven, and commercial cities had not yet developed. The results of the Lorenz curve and Moran analyses showed that the distribution of urban systems in China during the traditional period had a nonuniform spatial distribution of agglomeration.

(3) Large-scale military topographic maps of historical periods have proven to be a good source for land use reconstruction. Uncertainty analysis showed that the military topographic maps for the 1930s have good accuracy, and the correlation coefficient between the reconstructed urban areas based on topographic maps and the area values obtained using remote sensing images was 0.976. The $1° \times 1°$ gridded urban land area dataset constructed based on a GIS model of the TCE is important for future research on historical LUCC and can provide basic data for climate change models, urban economic history, and other disciplines.

Author Contributions: Conceptualization, Z.W. and H.W.; methodology, Z.W.; software, H.W.; validation, Z.W.; formal analysis, H.W.; investigation, Z.W.; resources, Z.W.; data curation, Z.W.; writing—original draft preparation, Z.W.; writing—review and editing, H.W.; visualization, Z.W.; supervision, H.W.; project administration, H.W.; funding acquisition, H.W. All authors have read and agreed to the published version of the manuscript.

Funding: This research was funded by National Social Science Fund of China (20VJXT004).

Institutional Review Board Statement: This study did not involve human or animals.

Informed Consent Statement: Informed consent was obtained from all subjects involved in this study.

Data Availability Statement: The data are contained within this article.

Acknowledgments: We thank LetPub (www.letpub.com, accessed on 13 December 2022) for its linguistic assistance during the preparation of this manuscript.

Conflicts of Interest: The authors declare no conflict of interest.

References

1. Proctor, J.D. The meaning of global environmental change: Retheorizing culture in human dimensions research. *Glob. Environ. Chang.* **1998**, *8*, 227–248. [CrossRef]
2. Lambin, E.F.; Turner, B.L.; Geist, H.J.; Agbola, S.B.; Angelsen, A.; Bruce, J.W.; Coomes, O.T.; Dirzo, R.; Fischer, G.; Folke, C. The causes of land-use and land-cover change: Moving beyond the myths. *Glob. Environ. Chang.* **2001**, *11*, 261–269. [CrossRef]
3. Houet, T.; Loveland, T.R.; Hubert-Moy, L.; Gaucherel, C.; Napton, D.; Barnes, C.A.; Sayler, K. Exploring subtle land use and land cover changes: A framework for future landscape studies. *Landsc. Ecol.* **2010**, *25*, 249–266. [CrossRef]
4. Fu, C. Potential impacts of human-induced land cover change on East Asia monsoon. *Glob. Planet. Chang.* **2003**, *37*, 219–229. [CrossRef]
5. Bae, J.; Ryu, Y. Land use and land cover changes explain spatial and temporal variations of the soil organic carbon stocks in a constructed urban park. *Landsc. Urban Plan.* **2015**, *136*, 57–67. [CrossRef]
6. Mather, A.S.; Needle, C.L.; Fairbairn, J. The human drivers of global land cover change: The case of forests. *Hydrol. Process.* **1998**, *12*, 1983–1994. [CrossRef]
7. Uhrqvist, O.; Lövbrand, E. Rendering global change problematic: The constitutive effects of Earth System research in the IGBP and the IHDP. *Environ. Polit.* **2014**, *23*, 339–356. [CrossRef]
8. Brunn, S.D.; O'Lear, S.R. Research and communication in the invisible college of the Human Dimensions of Global Change. *Glob. Environ. Chang.* **1999**, *9*, 285–301. [CrossRef]
9. Steffen, W. Introducing the Anthropocene: The human epoch. *Ambio* **2021**, *50*, 1784–1787. [CrossRef]
10. Fang, X.; Zhao, W.; Zhang, C.; Zhang, D.; Wei, X.; Qiu, W.; Ye, Y. Methodology for credibility assessment of historical global LUCC datasets. *Sci. China Earth Sci.* **2020**, *63*, 1013–1025. [CrossRef]
11. Alverson, K.; Oldfield, F. Pages: Past global changes and their significance for the future: An introduction. *Quat. Sci. Rev.* **2000**, *19*, 3–7. [CrossRef]
12. Newman, L.; Kiefer, T.; Otto-Bliesner, B.; Wanner, H. The science and strategy of the Past Global Changes (PAGES) project. *Curr. Opin. Environ. Sustain.* **2010**, *2*, 193–201. [CrossRef]
13. Morrison, K.D.; Tello, E.; Hammer, E.; Popova, L.; Madella, M.; Whitehouse, N.; Gaillard, M. Global-scale comparisons of human land use: Developing shared terminology for land-use practices for global change. *Past Glob. Chang. Mag.* **2018**, *26*, 8–9.
14. Ioannides, Y.M.; Zhang, J. Walled cities in late imperial China. *J. Urban Econ.* **2017**, *97*, 71–88. [CrossRef]
15. Ramankutty, N.; Foley, J.A. Characterizing patterns of global land use: An analysis of global croplands data. *Glob. Biogeochem. Cycles* **1998**, *12*, 667–685. [CrossRef]
16. Ramankutty, N.; Foley, J.A. Estimating historical changes in global land cover: Croplands from 1700 to 1992. *Glob. Biogeochem. Cycles* **1999**, *13*, 997–1027. [CrossRef]
17. Klein Goldewijk, K.; Beusen, A.; Van Drecht, G.; De Vos, M. The HYDE 3.1 spatially explicit database of human-induced global land-use change over the past 12,000 years. *Glob. Ecol. Biogeogr.* **2011**, *20*, 73–86. [CrossRef]
18. Klein Goldewijk, K.; Beusen, A.; Janssen, P. Long-term dynamic modeling of global population and built-up area in a spatially explicit way: HYDE 3.1. *Holocene* **2010**, *20*, 565–573. [CrossRef]
19. He, F.; Li, M.; Li, S. Reconstruction of Lu-level cropland areas in the Northern Song Dynasty (AD976-1078). *J. Geogr. Sci.* **2017**, *27*, 606–618. [CrossRef]
20. Li, S.; He, F.; Zhang, X. A spatially explicit reconstruction of cropland cover in China from 1661 to 1996. *Reg. Environ. Chang.* **2016**, *16*, 417–428. [CrossRef]
21. Liu, M.; Tian, H. China.s land cover and land use change from 1700 to 2005: Estimations from high-resolution satellite data and historical archives. *Glob. Biogeochem. Cycles* **2010**, *24*, 1–18. [CrossRef]
22. Ge, Q.; Dai, J.; He, F.; Zheng, J.; Man, Z.; Zhao, Y. Spatiotemporal dynamics of reclamation and cultivation and its driving factors in parts of China during the last three centuries. *Prog. Nat. Sci.* **2004**, *14*, 605–613. [CrossRef]

23. He, F.; Ge, Q.; Zheng, J. Reckoning the Areas of Urban Land Use and Their Comparison in the Qing Dynasty in China. *Acta Geogr. Sin.* **2002**, *57*, 709–716.
24. He, F.; Li, S.; Zhang, X.; Ge, Q.; Dai, J. Comparisons of cropland area from multiple datasets over the past 300 years in the traditional cultivated region of China. *J. Geogr. Sci.* **2013**, *23*, 978–990. [CrossRef]
25. Zheng, J.; Lin, S.; He, F. Recent progress in studies on land cover change and its regional climatic effects over China during historical times. *Adv. Atmos. Sci.* **2009**, *26*, 793–802. [CrossRef]
26. Wan, Z.; Chen, X.; Ju, M.; Ling, C.; Liu, G.; Liao, F.; Jia, Y.; Jiang, M. Reconstruction and Pattern Analysis of Historical Urbanization of Pre-Modern China in the 1910s Using Topographic Maps and the GIS-ESDA Model: A Case Study in Zhejiang Province, China. *Sustainability* **2020**, *12*, 537. [CrossRef]
27. Pan, W.; Man, Z. The grid methods of drainage density data reconstruction in big river delta: Based on the case of Qingpu, Shanghai, 1918-1978. *J. Chin. Hist. Geogr.* **2010**, *25*, 5–14.
28. Chen, L.; Wang, Y. The profile of some military topographic map before 1949. *Hubei Arch.* **1999**, *13*, 31–32.
29. Yang, X.; Jin, X.; Lin, Y.; Han, J.; Zhou, Y. Review on China's spatially-explicit historical land cover datasets and reconstruction methods. *Prog. Geogr.* **2016**, *35*, 159–172.
30. Jin, X.; Cao, X.; Du, X.; Yang, X.; Bai, Q.; Zhou, Y. Farmland dataset reconstruction and farmland change analysis in China during 1661-1985. *J. Geogr. Sci.* **2015**, *25*, 1058–1074. [CrossRef]
31. Wan, Z.; Jia, Y.; Jiang, M.; Liu, Y.; Hong, Y.; Lu, C. Reconstruction of urban land use and urbanization level in Jiangxi Province during the Republic of China period. *Acta Geogr. Sin.* **2018**, *73*, 550–561.
32. Jiang, W. The urban form of traditional mid-small cities: Focus on cadastral maps of Jurong county town in the Republic China. *J. Chin. Hist. Geogr.* **2014**, *29*, 33–45.
33. Ren, Y.; Deng, F. Analysis of Cartographic Source Based on Map Integration of One in 50 000 in Mainland China. *Chin. Hist. Geogr.* **2020**, *40*, 132–142.
34. Jiang, W. Number of Commercial Towns in Jiangnan:A Sharp Contrast of the Number of Commercial Towns between Changshu and Wujiang. *J. Chin. Hist. Geogr.* **2017**, *32*, 56–69.
35. Zhou, Z. *General History of China's Administrative Divisions*; Fudan University Press: Shanghai, China, 2007; pp. 1–785.
36. Zhang, Y. *History of Chinese Cities*; Baihua Literature and Art Publishing House: Tianjin, China, 2003; pp. 1–605.
37. Xie, J.; Jin, X.; Lin, Y.; Cheng, Y.; Yang, X.; Bai, Q.; Zhou, Y. Quantitative estimation and spatial reconstruction of urban and rural construction land in Jiangsu Province, 1820-1985. *J. Geogr. Sci.* **2017**, *27*, 1185–1208. [CrossRef]
38. Cheng, Y. The Urban Size and Administrative Scales in the Qing Dynasty. *J. Yangzhou Univ.* **2007**, *11*, 124–128.
39. Whitehand, J.; Gu, K. Urban conservation in China: Historical development, current practice and morphological approach. *Town Plan. Rev.* **2007**, *78*, 643–670. [CrossRef]
40. Chen, Y. Modeling fractal structure of city-size distributions using correlation functions. *PLoS ONE* **2011**, *6*, e24791. [CrossRef]
41. Chen, Y.; Zhou, Y. Multi-fractal measures of city-size distributions based on the three-parameter Zipf model. *Chaos Solitons Fractals* **2004**, *22*, 793–805. [CrossRef]
42. Benguigui, L.; Czamanski, D. Simulation Analysis of the Fractality of Cities. *Geogr. Anal.* **2004**, *36*, 69–85. [CrossRef]
43. Chen, Y.; Zhou, Y. The rank-size rule and fractal hierarchies of cities: Mathematical models and empirical analyses. *Environ. Plan. B* **2003**, *30*, 799–818. [CrossRef]
44. Feng, J.; Chen, Y. Spatiotemporal evolution of urban form and land-use structure in Hangzhou, China: Evidence from fractals. *Environ. Plan. B: Plan. Des.* **2010**, *37*, 838–856. [CrossRef]
45. Small, C. Global population distribution and urban land use in geophysical parameter space. *Earth Interact* **2004**, *8*, 1–18. [CrossRef]
46. Li, N.; Wang, J.; Wang, H.; Fu, B.; Chen, J.; He, W. Impacts of land use change on ecosystem service value in Lijiang River Basin, China. *Environ. Sci. Pollut. R.* **2021**, *28*, 46100–46115. [CrossRef]
47. Ord, J.K.; Getis, A. Local spatial autocorrelation statistics: Distributional issues and an application. *Geogr. Anal.* **1995**, *27*, 286–306. [CrossRef]
48. Getis, A.; Ord, J.K. The analysis of spatial association by use of distance statistics. *Geogr. Anal.* **1992**, *24*, 189–206. [CrossRef]
49. Xu, X.; Zhou, Y.; Ning, Y. *Urban Geography*; Higher Education Press: Beijing, China, 2009; pp. 1–355.